Mapping of stress raising in laser clad components depending on geometry and defects

A. F. H. Kaplan[1*], M. M. Alam[1], J. Tuominen[2], P. Vuoristo[2], J. Miettinen[3], J. Poutala[3], J. Näkki[2,4], J. Junkala[4], Z. Barsoum[5]

[1]Luleå University of Technology, Dept. of Engineering Sciences and Mathematics, SE-971 87 Luleå, Sweden
[2]Tampere University of Technology, Department of Materials Science, FI-33101 Tampere, Finland
[3]Tampere University of Technology, Department of Engineering Design, FI-33101 Tampere, Finland
[4]Technology Centre KETEK Ltd, FI-67100 Kokkola, Finland
[5]Royal Institute of Technology, Department of Aeronautical and Vehicle Engineering, SE-100 44 Stockholm, Sweden
*Corresponding author: alexander.kaplan@ltu.se

Abstract

The fatigue life of laser clad components is basically determined by stress raisers, which are here studied by Finite Element Analysis. Cylindrical and square section bars are compared for axial, bending and torsional load conditions, which induces the macro-stress field with corresponding stress peaks. The here presented material is an extension of previously published results, particularly with respect to defects in the clad layer, crack initiation sites and crack propagation paths. Defects from laser cladding such as pores, cracks or the surface roughness superimpose additional stress raising action on this stress field. The geometrical position and orientation of the defects has strong impact on the induced maximum stress level. For surface pores it is demonstrated by the fractography that their occurrence within a critical azimuthal range can initiate fatigue cracking. The different conditions of sample geometry, load situations, materials and defects are compared and discussed. In particular, advanced illustration methods are applied for improved and generalized documentation and explanation of the trends, both qualitatively and quantitatively. Guidelines are presented, in particular emphasizing critical defects and situations, such as surface pores that are difficult to detect because of inclusions, or pores just underneath the surface that generate particularly high stress.

Keywords: laser cladding, defect, geometry, fatigue cracking, stress raiser

1 Introduction

Fatigue cracking of laser clad components takes place from locations of maximum stress. These locations depend on the macroscopic stress load of a certain component under specific load plus local stress raisers, particularly by defects like pores or cracks. A literature survey on defects and fatigue cracking of laser cladding was written by Md. M. Alam [1]. The present study compares four different basic laser clad components and their load case as well as different defects and their location and orientation. Comparison between the different stress raisers is illustrated by various documentation methods. Experimental results from fatigue fractography confirm their origin from stress raisers like pores. While part of the results have already been published,[1-6] we here complement earlier results and survey maps with additional new results on laser clad imperfection types and on the fatigue crack initiation. The here presented results are an extension of a recently published paper.[5]

2 Methodology

Four basic laser clad component geometries with corresponding load conditions are studied, namely (i) a cylindrical rod for axial load, (ii) a cylindrical rod for four-point bending load, (iii) a rectangular bar for four-point bending load and (iv) a cylindrical rod for torsional load. The circular rods are laser-clad at the entire surface while the rectangular bar is laser-clad at one side. After laser-cladding, for optimized parameters, the clad surfaces are smoothened by machining off a layer. Visual inspection is carried out for the detection of surface defects, particularly pores. The clad components are fatigue tested, to develop SN-diagrams, also in comparison with non-clad base material samples. Stress analysis by the Finite Element Method, FEM, is carried out to calculate the stress field for the respective load condition of the components, called the macro-field. In addition, local stress analysis of defects is performed, which is an additive stress raiser to the macro-field in its respective location. For certain situations the crack propagation is also calculated by FEA. Fractography by microscopic analysis of the fracture surfaces of the samples after fatigue testing provides additional information. Occasionally, cross sections of the laser clads are made, to study the metallurgy and defects, accompanied by other kinds of analysis, including residual stress measurement. Finally, the main trends are interpreted, categorized and visualized in graphical charts.

2.1 Laser cladding

Laser cladding was carried out at the Technology Centre KETEK Ltd. in Kokkola, Finland, with the parameters shown in Table 1. A diode-pumped Nd:YAG-laser was used. A 1.5 mm thick clad layer was made, machined off then to 0.75 mm. More details can be found in [2-6].

Table 1. Parameters used for laser cladding

Parameter	Value / Unit
Laser beam power (cw)	3.25 kW
Beam diameter	6 mm
Traverse speed	1.1 m/min
Powder feeding rate	30 g/min
Shielding gas type	Ar
Gas flow rate	16 l/min
Lateral clad layer displacement	2 mm

2.2 Fatigue testing

The fatigue testing was carried out at different locations of the Finnish partners. The four different loading situations described above were tested, i.e. axial, bending (cylindrical rod and rectangular bar) and torsional fatigue load. Details about the fatigue testing set-up and results can be found in [1-6]. As example, Fig. 1(a) shows a cracked cylindrical rod after four-point bending fatigue testing. Beside the primary crack also a secondary crack can be seen. A cross section of the milled laser clad is shown in Fig. 1(b) where the vertical crack (here the secondary crack, denominated E) through the clad layer into the substrate can be seen. Note the wavy interface clad-substrate from the overlapping clad-layers. The crack surface of the rod can be seen in Fig. 1(c). The fatigue testing was stopped after a certain crack propagation and drop in force and strain and the sample was cut through afterwards. In this case it was

found that the crack was initiated from a surface pore that was filled with an oxide inclusion, see Figs. 1(d)-(f), which is described in detail in [3].

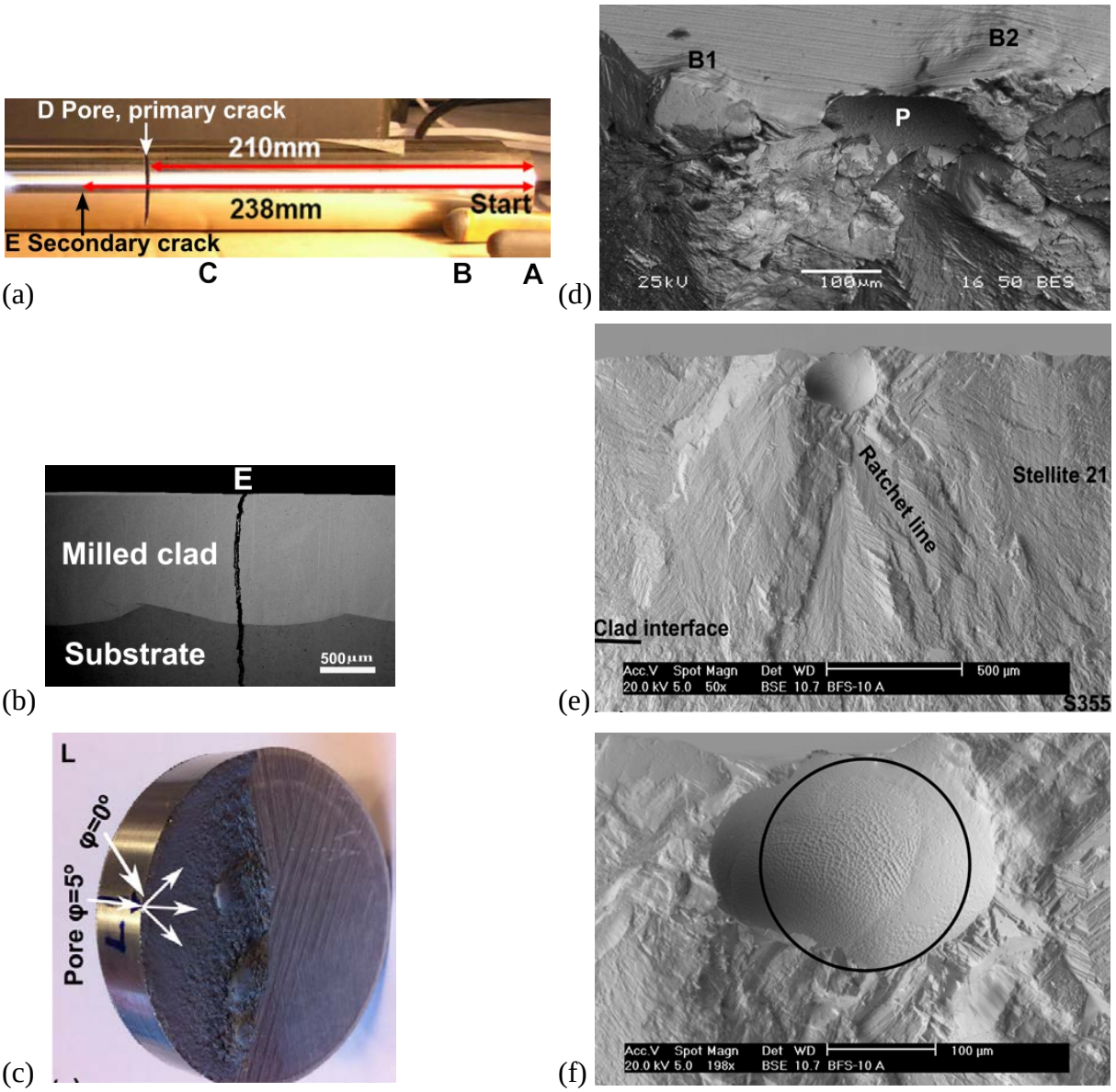

Fig. 1. (a) 2 cracks at round rod (here non-clad, for comparison) after four-point bending fatigue testing, (b) secondary crack through the clad layer, (c) fracture surface of the rod with pore location as crack initiation, (d)-(f) surface pore and crack surface with ratchet lines.

2.3 FE stress analysis

Stress analysis was carried out at different levels, by Finite Element Analysis, FEA. The static stress field, the macro-field, was calculated for the maximum load of the four cases. For a variety of defect geometries (pores, surface pores, hot cracks, etc.) the stress raiser or stress concentration factor K was calculated locally around the defect. Moreover, the stress raisers were superimposed to the calculated macro-field to study the influence of different locations and orientations of defects in the component. In addition, the crack propagation was calculated (simplified in two dimensions) by FEA, based on the stress intensity KI at the tip of the crack, leading to the direction and speed of the fatigue crack propagation but also

indicating its preferred location of initiation, from maximum stress raisers. In particular, the stress propagation was computed for different locations of initiation, for different sizes and orientations of initiation defects and for different interaction when propagating in the vicinity of defects. Details of the stress analysis method, i.e. the FEA can be found in [1-5]. From the stress analysis, better interpretation of the experimental results has been expected.

The study tries to distinguish between the stress field induced by the load including defect stress raisers and the residual stress field as a different mechanism to be optimized. The residual stress field was measured for a few samples.

3 Results and discussion

3.1 Macro stress field depending on load

The calculated macro-stress field for the four cases studied is shown in Fig. 2.

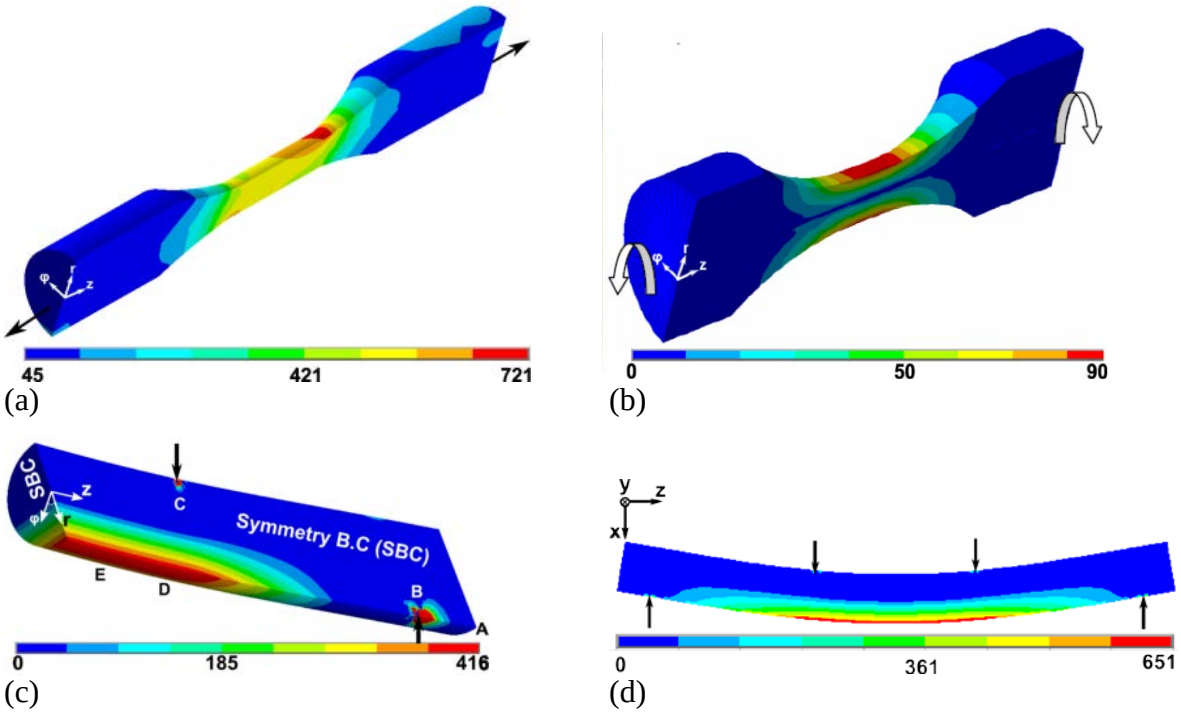

Fig. 2. Calculated 1st principle macro stress field (in MPa, long section) for (a) axial fatigue loading of a cylindrical laser clad rod, (b) torsional loading (cylindrical), (c) 4-point bend load (cylindrical, here quarter-rod), (d) 4-point bend load (rectangular bar, bottom-clad).

For the axial and torsional load a 'dog-bone'-geometry was used, following the standards. For axial loading, the representative cylindrical central part shows an almost constant stress value. Torsional load leads to a central (red) peak around the cylinder, rapidly decaying radially inwards, as shear stress slices. For bending load a long area of rather constant maximum stress is obtained at the lower surface, strongly decreasing upwards. This macro field (note: it is the amplitude of the cyclic fatigue load) is the starting condition for the loaded laser-clad component, so far without any imperfections at the surface or in the material. Fatigue cracking is expected to initiate from the respective peak stress location. The material plays here a minor role [2] because the E-modulus of the thin clad and the base material match well.

3.2 Defects as stress raisers

Figure 3 shows a variety of possible defects from laser cladding, and examples for different locations and orientations of these defects, both for the as-clad surface and when machining off a layer to a smooth surface. From the geometrical nature of the defects it can be distinguished between 0-dimensional defects like pores or inclusions, 1-dimensional defects like the ripples from the as-clad surface or the wavy interface clad-substrate, and defects extended in two dimensions like lack-of-fusion or hot cracks. Photographs of different laser clad defects obtained can be seen in Fig. 4.

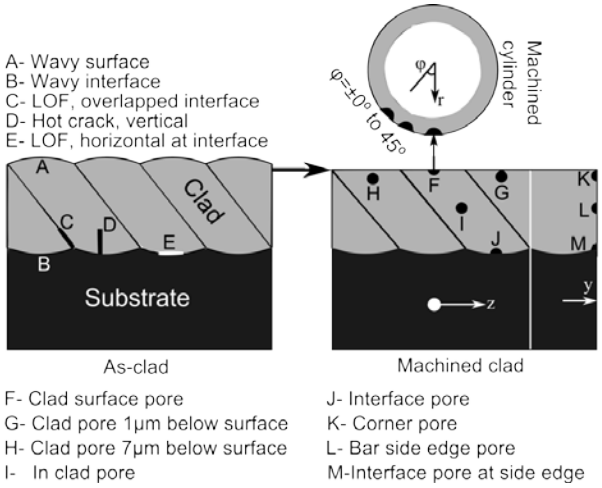

Fig. 3. Illustration of the laser clad layer cross section (left as-clad and right after machining) with the variety of possible defects and their positions

For some of the defects in Fig. 4, extensive numerical stress analysis was carried out, see Fig. 5, in order to qualitatively and quantitatively assess their stress raiser role. For a certain location of a defect, the corresponding stress level from the macro stress field is the local reference environment for stress raised by the defect shape. The three categories of defects are defined through their geometrical extensions. They correspondingly experience a point (0D), linear (1D) or planar (2D) macro stress field. For example, Figure 5(e),(f) shows the calculated stress field (note: different scale) at a spherical pore, when located just underneath the surface or as surface pore, i.e. representative also for the cracking shown in Fig. 1. More discussions and more calculated stress fields for laser clad defects as stress raisers and comprehensive analysis can be found in [2,3,5]. One conclusion is that a pore just underneath the surface is the strongest stress raiser. Moreover, a central location as in Fig. 1(c) is the most critical azimuthal location.

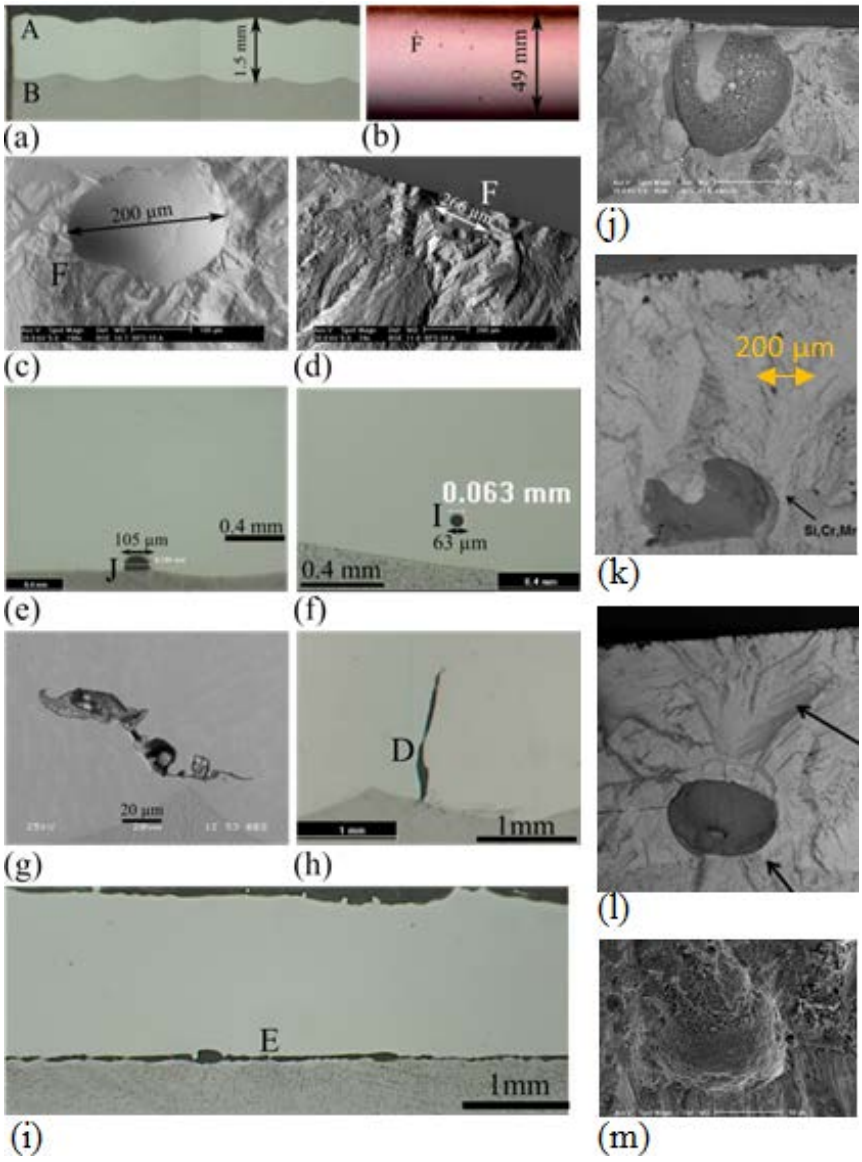

Fig. 4. Photographs of laser cladding defects; (a) as-clad wavy surface A and interface B, (b) detection of surface pores F by dye penetration test, (c) surface pore F, (d) surface pore F with oxide inclusion, (e) semi-spherical interface pore J between clad layer and base material, (f) spherical pore I in-clad, (g) irregular inclusion near the interface, (h) hot crack D, (i) interface lack-of-fusion E; (j) surface pore with oxide inclusion F, (k,l) interface pore with oxide inclusion J, (m) inner pore I with traces of Cr-oxide.

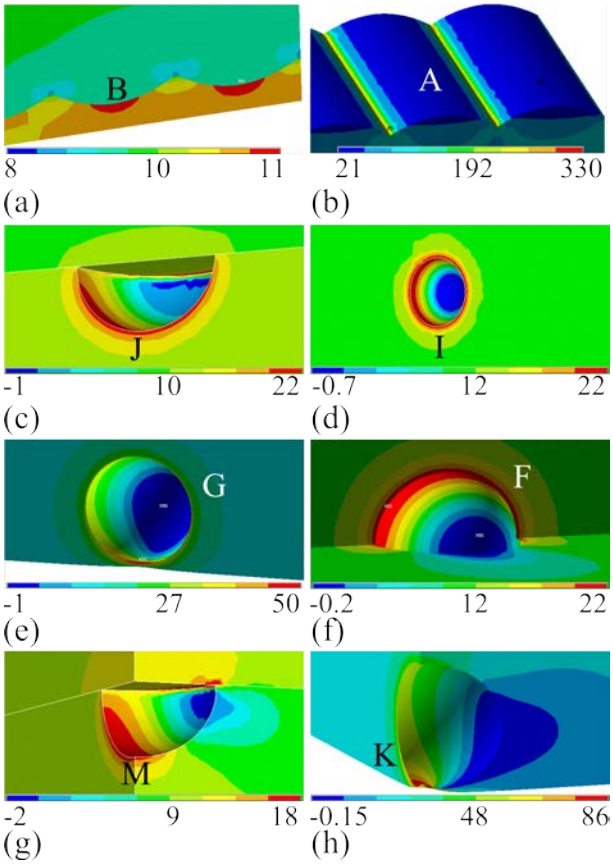

Fig. 5. Local 1st principle stress field (in MPa) for various laser clad defects; (a) wavy interface clad-substrate B, (b) as-clad wavy surface A, (c) semi-spherical interface pore clad/substrate J, (d) spherical in-clad pore I, (e) spherical in-clad pore G buried 1 µm underneath the surface, (f) semi-spherical surface pore F, (g) interface pore M half open at the side edge, (h) pore K half open at the side edge and 1 µm underneath the top surface.

3.3 Crack propagation

In the following, macrographs of the fracture surface are presented, to present typical fracture surfaces, including the crack initiation locations and crack propagation directions. When the crack initiation was associated with a defect, the defects and the local fracture pattern is shown in detail for a series of examples. Figure 6(a),(b) shows an example (for a cylindrical rod that was 4-point fatigue bent) of the two fracture surfaces where a pore with oxide inclusion at the clad surface was located close to the most critical azimuthal location. The fracture propagates clearly from this crack initiation site. This example of evidence was evaluated and discussed in detail by Alam et al. [3]. In Fig. 6(c) can be seen that one fracture surface can have experienced several defects distributed at different azimuthal angles of the laser clad layer. The cracking then propagates from several defects simultaneously, particularly if they are within the (generally valid) critical range of azimuthal angles of ±55° which was derived by Alam [3]. On some samples many surface defects were detected, as shown in Fig. 6(d). A secondary and tertiary crack was initiated from two defects located closely to the primary crack, towards the centre of the rod, i.e. where the stress keeps high, see also Fig. 2(c).

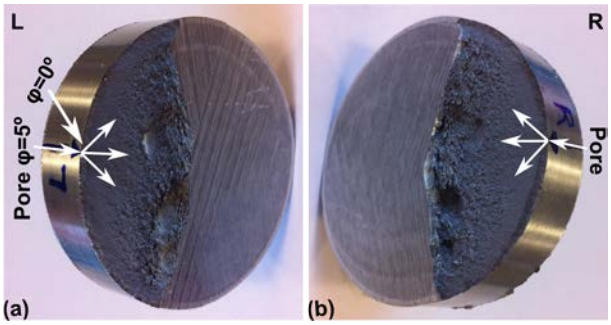

(c)

(d)

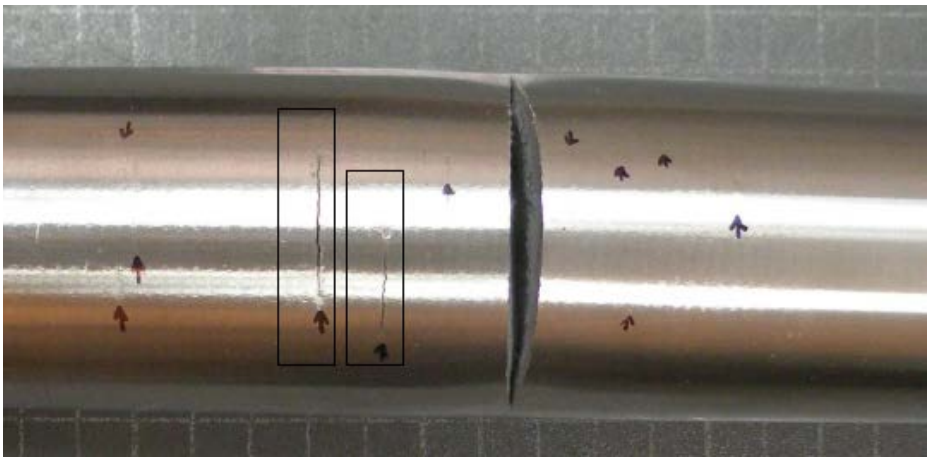

Fig. 6: Locations of defects at a cylindrical rod: (a),(b) pore almost at azimuthal position φ=0 of maximum stress, initiating primary cracking; (c) numerous defects (arrows) at different azimuthal positions of the fracture surface border; (d) defects marked at the rod surface, including two defects initiating secondary and tertiary cracking (rectangles)

The crack initiation and propagation for cylindrical rods just of the base metal (here 42CrMo4) is shown in Fig. 7, again for 4-point bending. In Fig. 7(a),(b) the crack propagates from the surface, roughly from the location of maximum stress, as can be expected. As can be seen in detail, Fig. 7(c), no surface defects were detected (just local deformation), according to the well prepared base metal samples. Interesting is that cracking can be initiated in the bulk of the rod instead, see Fig. 7(d), although no defect was found either.

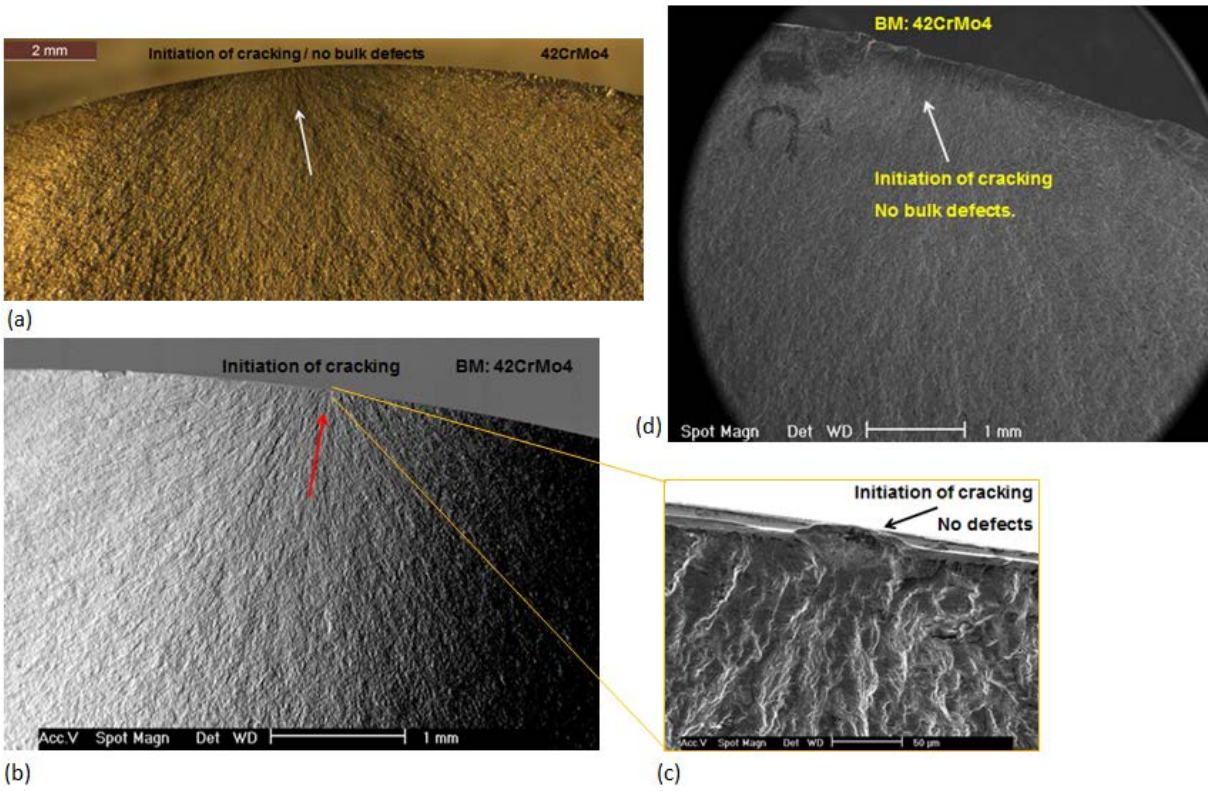

Fig. 7: Fracture surface with crack initiation and propagation in the base metal (BM: 42CrMo4) of a cylindrical rod without clad under 4-point bending: (a),(b) surface initiation, (c) magnified location of initiation (no surface defect), (d) initiation in the bulk, no defect

For rods with laser clads, typical fractography photos can be seen in Fig. 8. Completely defect-free clads were difficult to achieve. Accordingly, the fracture initiation was often initiated by a defect, like by a surface pore with oxide inclusion, as in Fig. 8(a) (Inconel 625 clad layer) or Fig. 8(d) (Stellite 21 clad layer). Note that pores just underneath the surface, or slightly opened raise a higher stress than more open pores and are hence much more critical, as was studied deeper and explained by FEA [2,3]. Figures 8(b),(c) show that the cracking can initiate from several locations and then generates several propagation paths. In Fig. 8(b) a pore inside the clad layer, type I in Fig. 3, generated cracking which was more seldom than surface pores F or interface pores J.

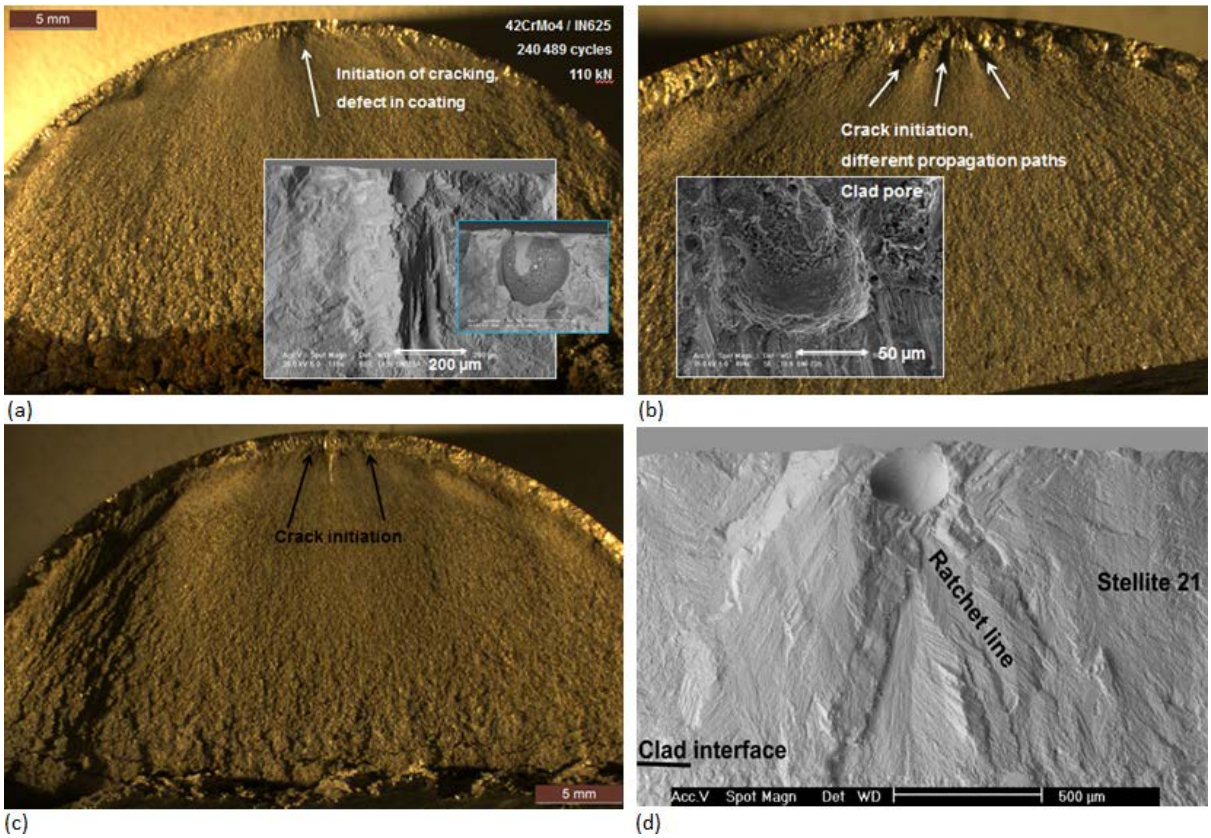

Fig. 8: Crack propagation pattern of laser clad rods and location of crack initiation: (a) initiation by a surface pore with oxide inclusion, F, close to the azimuthal peak stress, (b) different propagation paths and pore in the clad layer, I, (c) different crack initiation sites, (d) pore underneath the surface, F, that initiated the crack propagation

A closer view on pores with inclusions and on the surrounding fractography is shown in Fig. 9. Figure 9(a) shows a crack interface pore filled with oxide from which the brittle fracture initiated and propagated both upwards to the surface and radially into the centre of the rod. Figure 9(b) shows another surface pore filled with oxide from which the crack initiated, similar to Fig. 1 and Fig. 8. Fracture from another interface pore with inclusion is shown in Fig. 9(c). The pore boundary is flat towards the interface. Slippery bands can be found close to the defect.

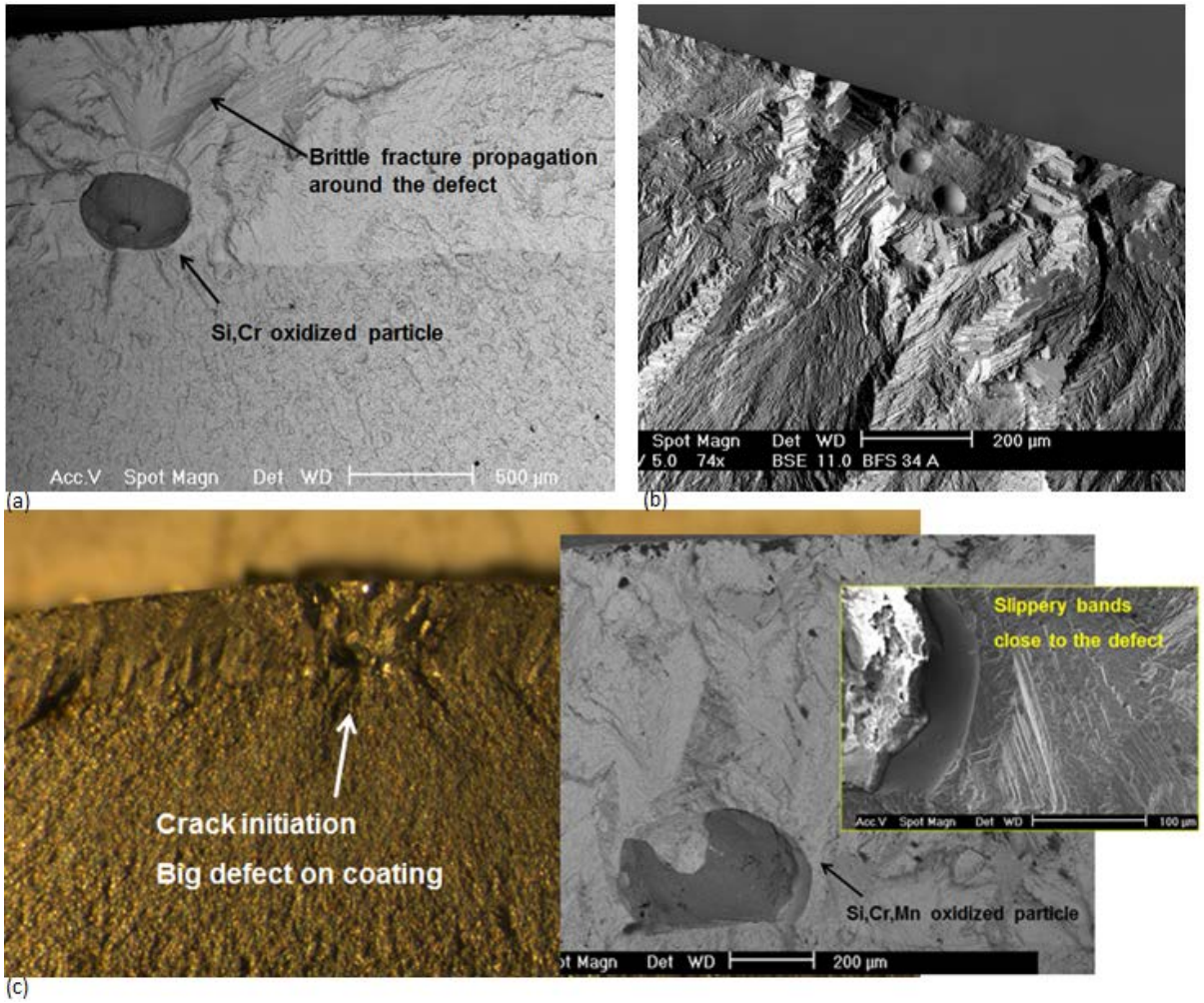

Fig. 9: Clad layer defects initiating cracking: (a) pore with oxide inclusion at the clad-substrate interface, J, with propagations to top and centre, (b) surface pore with oxide inclusion, F, that initiated cracking, (c) pore with oxide at the interface, J, showing slippery bands and initiating cracking

More details of fractography are shown in Fig. 10. Fatigue striations can be seen in Fig. 10(a), corresponding to an advancement rate of the crack by about 18 µm/cycle. In Fig. 10(b) a hole that requires an according pile of slippery bands can be seen in the coating from which cracking might have been initiated. Figure 10(c) shows a deviated cracking path (ratchet line) that might indicate crack initiation in the middle of the clad layer. Crack initiation underneath a pore can be seen in Fig. 10(d). The fractography analysis supports the understanding of the crack initiation and propagation and enables improved judgment of how critical a certain defect is and its impact on initiation and propagation.

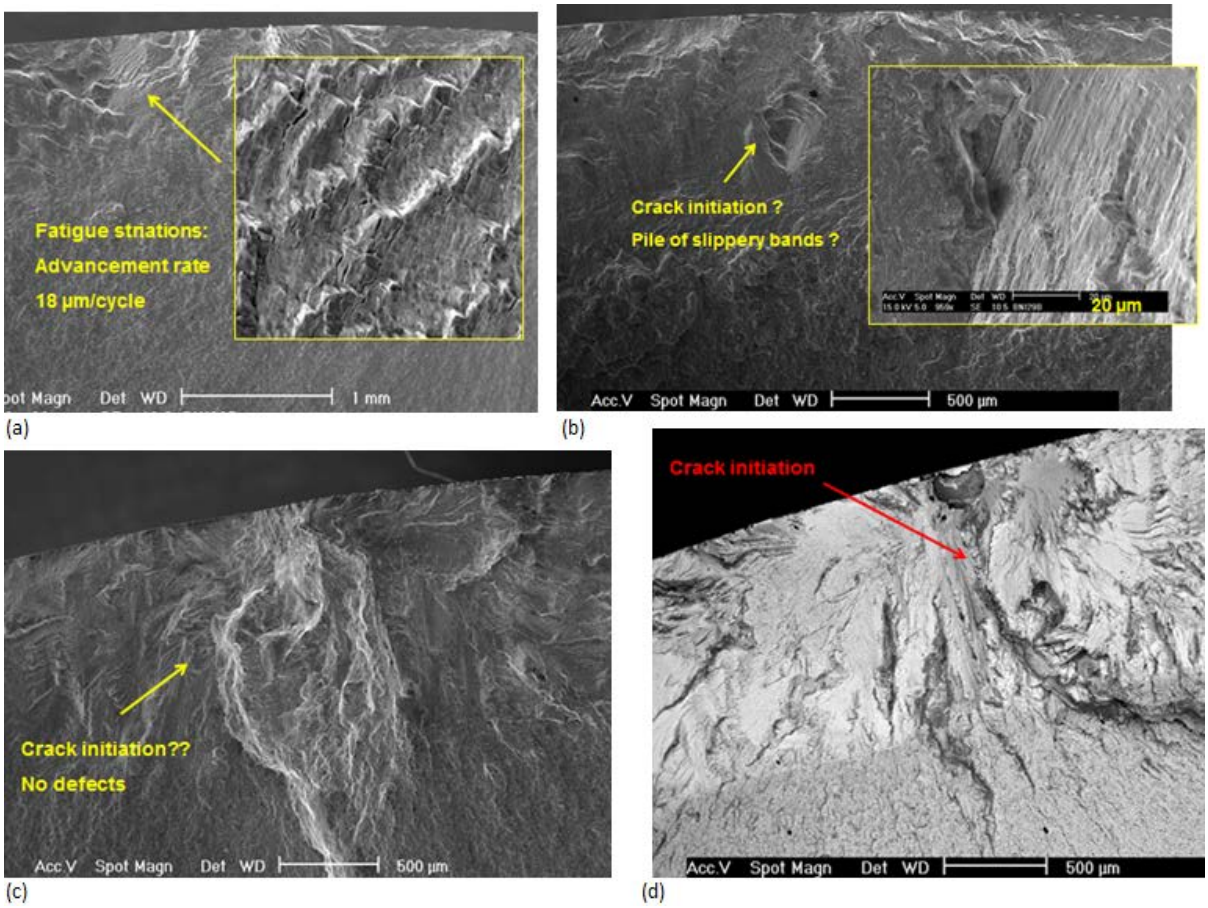

Fig. 10: Locations of crack initiation: (a) fatigue step striation pattern, (b) hole/pile of slippery propagation bands, (c) non-straight propagation path, without defect, (d) crack initiation underneath a surface pore, F

3.4 Survey maps as guidelines

The trends of the two overlapping mechanisms, namely the macro-field and the stress raiser defects are visualized in a quantitative manner in Fig. 11 and in a qualitative manner in Fig. 12, then called Tuning Flow Chart, TFC. The illustrations can be applied as guidelines and they can be extended in case of additional findings. In [1-6] the trends are explained and discussed and recommendations are given. Sometimes the size of the defect is of importance, but more often its location or orientation.

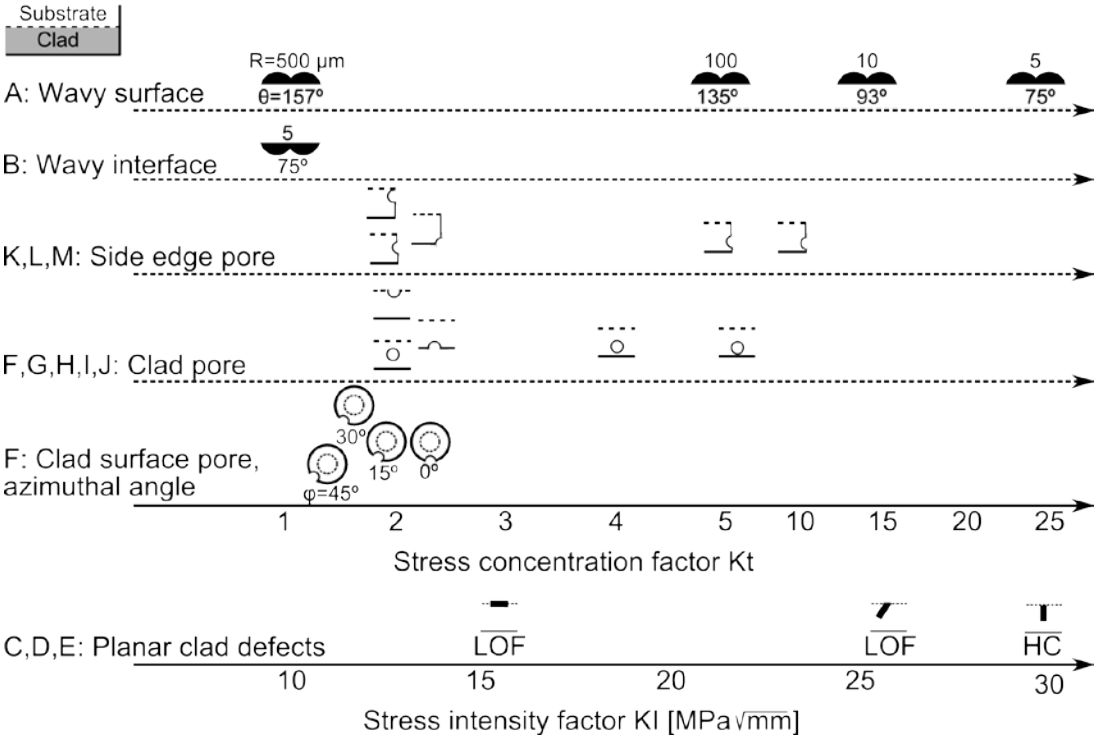

Fig. 11. Stress concentration factor and stress intensity factor for various clad defects and their geometry variations

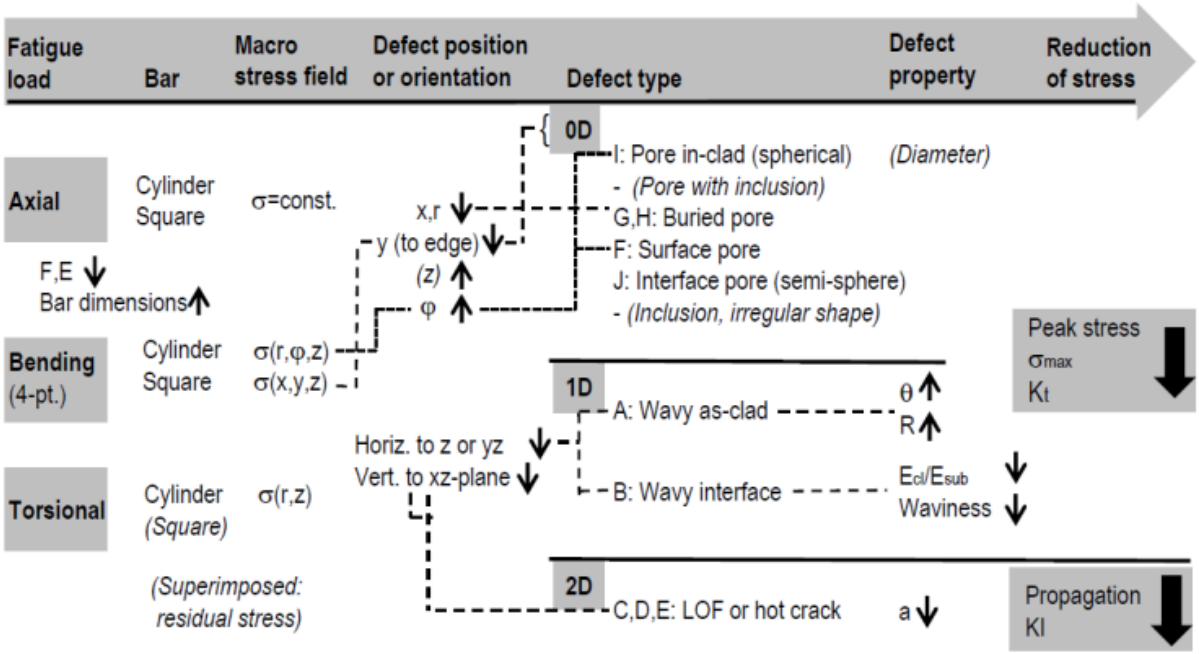

Fig. 12. Tuning Flow Chart, TFC, describing the combination of different stress raisers of laser clad bars under fatigue load; the arrows indicate lowering of the peak stress

4 Conclusions

For the theoretical study of stress raising and fatigue life in laser clad components the following conclusions can be drawn:

(i) The maximum stress in a laser- clad component, which is likely to initiate fatigue cracking, is generated from a superposition of:
   a. the macro-stress field (from load and component geometry),
   b. stress raisers by defects (from laser cladding),
   c. residual stress (generated during laser cladding).

(ii) Mainly tensile residual stress was measured, which can reduce the fatigue lifetime.

(iii) For defects, their location and orientation in the macro-field is often more important for their generation of stress raisers than the defect size.

(iv) Experimental evidence was found where surface and interface pores have initiated fatigue cracking.

(v) The visualizing maps developed enable to systematically extend existing knowledge and they facilitate the cognition of knowledge, here for stress raisers through defects.

5 Acknowledgements

The authors acknowledge funding from the EU regional development programme Interreg IVA Nord, project FATLASE, no. 304-13933-09.

6 References

[1] Alam, M. M.: Laser welding and cladding: The effects of defects on fatigue behaviour, PhD-thesis, Luleå University of Technology, Sweden (2012).

[2] Alam, M. M.; Kaplan, A. F. H.; Tuominen, J.; Vuoristo, P.; Miettinen, J.; Poutala, J.; Näkki, J.; Junkala, J.; Peltola, T.; Barsoum, Z.: Analysis of the stress raising action of flaws in laser clad deposits, Materials and Design, v. 46, p. 328-337 (2013).

[3] Alam, M. M.; Powell, J.; Kaplan, A. F. H.; Tuominen, J.; Vuoristo, P.; Miettinen, J.; Poutala, J.; Näkki, J.; Junkala J.; Peltola T.: Surface pore initiated fatigue failure in laser clad components, Journal of Laser Applications, v. 25, n. 3, p. 032004 (6 pages) (2013).

[4] Tuominen, J., Näkki, J., Poutala, J., Miettinen, J., Peltola, T., Vuoristo, P., Alam, M., Kaplan, A.: Fatigue properties of laser clad round steel bars, Proc. ICALEO, Miami (FL), LIA, Paper #P140 (2013).

[5] Kaplan, A. F. H., M. M. Alam, J. Tuominen, P. Vuoristo, J. Miettinen, J. Poutala, J. Näkki, J. Junkala, T. Peltola and Z. Barsoum: Stress raising in laser clad components depending on geometry and defects, Proc. NOLAMP 14, August 26-28, 2013, Gothenburg/Sweden (2013).

[6] Fantozzi, D.: Fatigue behaviour of Ni and Co laser cladded coatings on steel bars, Master thesis, University of Modena and Reggio Emilia, Italy (2013).